Quantum Simulation of Phenol−Water Clusters

David M. Benoit and David C. Clary*

Department of Chemistry, University College London, 20 Gordon St., London WC1H OAJ, U.K.

Received: December 17, 1999; In Final Form: March 9, 2000

We investigate the vibrational ground-state structure and energetics of phenol−$(H_2O)_n$ ($n = 2-5$) hydrogen-bonded clusters using the rigid-body diffusion quantum Monte Carlo method. We find that the complexes of small size ($n < 5$) are similar to related pure-water clusters $(H_2O)_{n+1}$ and that quantum zero-point effects influence their structure. We calculate the vibrational ground-state structure of phenol−$(H_2O)_5$ and show that π-hydrogen bonding between water and the aromatic cycle may be relevant in explaining unusual features of the experimental jet-cooled infrared spectrum.

I. Introduction

Phenol is the simplest prototype of an aromatic alcohol. Structurally, alcohols have some similarities to water but the substituent replacing one of the hydrogen atoms can induce interesting properties. In the case of phenol, the substituent is a phenyl ring, which places the phenol midway between a benzene molecule and a water molecule. This difference makes phenol a weak acid ($pK_a = 9.9$ in water), and therefore a better proton donor than water. Interaction of this molecule with water provides a useful system to analyze the competition between hydrophilic and hydrophobic solvation. Of particular interest is to examine the structure that phenol−$(H_2O)_n$ clusters take when n is varied.

Our previous quantum diffusion Monte Carlo study of both benzene−H_2O and phenol−H_2O gas-phase clusters[1] shows that a water molecule can be hydrogen bonded to a phenyl ring but prefers to be a proton acceptor in the presence of a phenol molecule (see Figure 1a). This is in contrast to benzene, which prefers to be a proton acceptor.

Recent experimental[2−7] and theoretical[8−13] studies suggest that the behavior of phenol in the gas phase is surprisingly similar to a water molecule; that is, only the −OH group is involved in hydrogen bonding (see Figure 1a,b, for example). This implies that phenol takes part in the formation of mixed cyclic clusters where the phenyl ring is not interacting significantly with any water molecules.

Courty et al.[14,15] experimentally, and Gregory et al.[16] theoretically, demonstrated that the bonding energy with which a benzene ring interacts with a water molecule is comparable in magnitude to a water−water hydrogen bond. The same type of π-hydrogen bond can occur between a phenol ring and a water molecule (see Figure 1c).

In addition, it is known that the monocyclic structure of pure-water clusters $(H_2O)_n$ exists for only up to five-membered rings. Liu et al.[17] and Gregory et al.[18,19] suggested that the water hexamer vibrational ground state has a three-dimensional polycyclic cage structure. In this cluster, three hydrogen bonds are weakened and therefore might be more susceptible to be broken to form stronger hydrogen bonds with an organic molecule, for example.

These two considerations imply that hydrated phenol might depart from water-like behavior when enough water molecules are allowed to interact with it. In other words, the presence of the phenyl ring in phenol should lead to the formation of a π-hydrogen bond with one of the surrounding water molecules when the cluster is flexible enough for the bond energy to compensate for the steric strain induced by the deformation of the hydrogen-bonded network. The existence of π-hydrogen bonding in many aromatic systems has been shown experimentally by, for example, X-ray diffraction[20] and microwave spectroscopy.[21,22]

Since Feller et al.[8] dismissed the existence of a π-hydrogen bonded isomer of phenol−water, on the grounds of their ab initio calculations, there has not been much theoretical work considering this structure as a significant isomer for phenol−$(H_2O)_n$. Whereas most model potentials exhibit a π structure, Feller's high quality ab initio computations could not characterize it as a stationary point. Nonetheless, Bürgi et al.[10] did mention the possibility of finding a π minimum structure in their ab initio study of the phenol−$(H_2O)_3$ complex. Later, in further ab initio calculations, Jacoby et al.[13] found a π minimum structure for the phenol−$(H_2O)_5$ cluster, which they named a "book" structure.

The relative energy of the isomers of phenol−$(H_2O)_n$ depends on the potential energy surface of the cluster and the dynamics of the monomers moving on this surface. Detailed calculations performed on pure-water clusters $(H_2O)_n$ (see ref 17, for example) show that vibrational zero-point energy effects are significant in determining the relative energies and vibrationally averaged geometries of the various isomers. The vibrations in these clusters involve wide-amplitude, strongly anharmonic, motion that cannot be treated accurately using harmonic approximations. This is an important consideration for the theoretical treatment of phenol−$(H_2O)_n$.

Quantum diffusion Monte Carlo (DMC) is a technique for calculating the ground state of a molecular system. It can be applied to many particles and, when applied to molecular vibrations, has been shown to deal with anharmonicity accurately.[23] Gregory et al.[18] successfully applied this method to compute the vibrational zero-point energy of water clusters. It is, therefore, an ideal method to apply to phenol−$(H_2O)_n$. In particular, the rigid-body form of DMC (RB-DMC), which was used in the water cluster studies by Gregory et al.,[18] is very powerful as it permits a treatment focusing on the intermolecular

* Corresponding author. E-mail: d.c.clary@ucl.ac.uk.

10.1021/jp994420q CCC: $19.00
Published on Web 05/20/2000

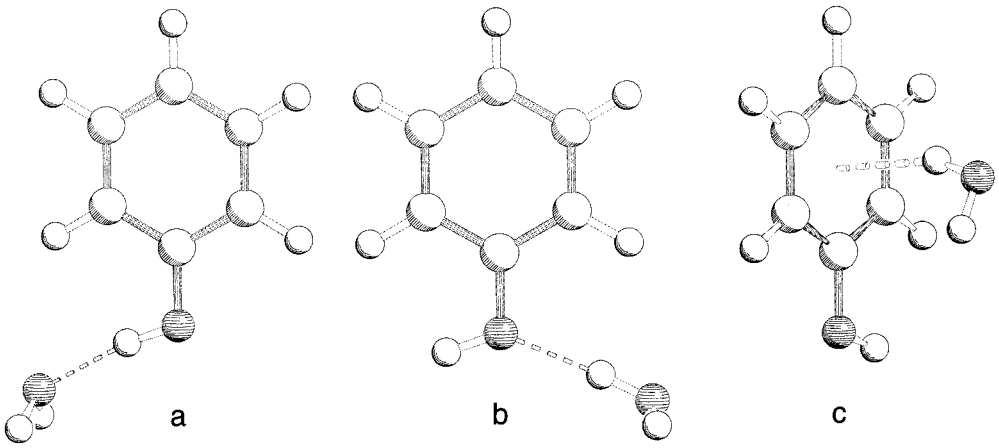

Figure 1. Three possible minima of the phenol−H_2O system on the OPLS surface. The phenol-donor structure (**1a**) is the global minimum, and the water-donor geometry (**1b**) is less stable; these two structures are similar to the ones found in water−water hydrogen bonding patterns. The third structure (**1c**) shows a π-minimum which is reminiscent of the benzene−water minimum structure.

vibrations and enables an efficient use of computer resources for many-dimensional problems.

So far, the structures of phenol−$(H_2O)_n$ (n = 2, 3, 4) have been identified by analogy to the parent $(H_2O)_n$ (n = 3, 4, 5) pure-water cluster. Both experiment and theory agree fairly well as to the nature of their respective vibrational spectra.[2−7] Note that in all these cases, the monomers adopt a pseudoplanar structure.

In the case of phenol−$(H_2O)_5$, where the analogous $(H_2O)_6$ water hexamer adopts a multicyclic three-dimensional structure, the experimental infrared spectrum contains extra features, which are assigned to a possible polycyclic form. The ab initio calculations of the IR spectrum published for this cluster[12,13] do not provide a complete match to the experimental data. Due to the high dimensionality of the cluster, it is possible that several isomers can contribute to the infrared spectrum. What is needed for a proper understanding of the cluster is a treatment of the vibrational states on the best available potential energy surface.

Here we apply the RB-DMC method to phenol−$(H_2O)_n$ (n = 2−5) complexes to determine their ground-state structure, dissociation energy (D_0), and rotational constants. We compare our results with available experimental data and examine in detail the importance of π-hydrogen bonding in these clusters. We also estimate the relative stability of the different isomers proposed and determine the extent of vibrational zero-point effects and nuclear delocalization. One aim of the work is to demonstrate the usefulness of the RB-DMC method for studying the hydration of organic molecules. In addition, we report ab initio calculations on some of the clusters and perform a vibrational frequency calculation at the density functional B3LYP/6-311++G(d,p) level of theory on selected minima of phenol−$(H_2O)_5$.

In section II, we summarize the basic principles of the diffusion Monte Carlo algorithm. The particular parameters and methods we use for the investigation of phenol−$(H_2O)_n$ complexes are introduced in section III. We present our results for phenol−$(H_2O)_n$ (n = 2−5) in section IV, and compare them with the most recent experimental findings. We draw our conclusions on this work in part V.

II. Quantum Diffusion Monte Carlo

Quantum diffusion Monte Carlo solves the Schrödinger equation by modeling a diffusion process in imaginary time on a given multidimensional potential energy surface. The numerically "exact" solution provided by this method takes full account of nuclear zero-point motion and quantum tunneling, giving information on the vibrational ground state of the system examined. This vibrationally averaged structure is a realistic picture of the cluster in a cold environment, such as a supersonic jet expansion, and the properties of the ground state calculated by this method have compared favorably with experiment.[17−19] Computational details of the algorithm have been reported elsewhere;[1,24−26] we are therefore only giving an outline of the method.

We can rewrite the time-dependent Schrödinger equation for a system of N particles, and introduce an energy-shifting term E_{ref}. By performing a Wick rotation, which transforms real time t into imaginary time $\pi = it$, we obtain

$$\hbar \frac{\partial \Psi(\vec{r},\tau)}{\partial \tau} = \sum_i^N \frac{\hbar^2}{2m_i} \nabla_i^2 \Psi(\vec{r},\tau) - [V(\vec{r}) - E_{ref}]\Psi(\vec{r},\tau) \quad (1)$$

The formal solution of this equation can be expanded in term of eigenfunctions of the time-independent Schrödinger equation $H\phi_j(\vec{r}) = E_j\phi_j(\vec{r})$ as follows:

$$\Psi(\vec{r},\tau) = \sum_{j=0}^{\infty} c_j \phi_j(\vec{r}) \exp\left[-\frac{(E_j - E_{ref})\tau}{\hbar}\right] \quad (2)$$

Then, if $E_{ref} = E_0$ and $c_0 \neq 0$, we have

$$\lim_{\pi \to \infty} \Psi(\vec{r},\tau) = c_0\phi_0(\vec{r}) \quad (3)$$

This shows that, within the above-mentioned conditions, any wave function $\Psi(\vec{r},0)$ can be relaxed to the ground state of the system if it is propagated long enough in imaginary time. It is useful to note that eq 1 is formally equivalent to a diffusion equation with an additional first-order rate term

$$\frac{\partial C(\vec{r},\tau)}{\partial \tau} = \sum_i^N D_i \nabla_i^2 C(\vec{r},\tau) - \frac{f(\vec{r})}{\hbar} C(\vec{r},\tau) \quad (4)$$

where $D_i = \hbar/2m_i$ is a mass-dependent diffusion constant, which arises from the translational kinetic energy. We can solve this equation by using a Green's function to propagate step by step the initial wave function $\Psi(\vec{r},0)$ in imaginary time. Mathematically, this can be written as

$$\Psi(\vec{r},\tau+\Delta\tau) = \int G(\vec{r} \rightarrow \vec{r}';\Delta\tau)\, \Psi(\vec{r}',\tau)\, \mathrm{d}^3\vec{r}' \qquad (5)$$

We use the following first-order short-time approximation to the Green's function, which can also be viewed as a infinitesimal evolution operator if $\Delta\tau$ is small

$$G(\vec{r}\rightarrow\vec{r}';\Delta\tau) = \prod_i^N \left(\frac{m_i}{2\pi\hbar\Delta\tau}\right)^{3/2} \exp\left[-\frac{m_i(\vec{r}-\vec{r}')^2}{2\hbar\Delta\tau}\right] \exp\left[-\frac{[V(\vec{r}) - E_{\mathrm{ref}}]\Delta\tau}{\hbar}\right] \qquad (6)$$

Note that the first part of the propagator defines the probability density of a Gaussian diffusion process and that the second term is a weighting factor related to the shifted potential energy.

The propagation of an initial wave function is then implemented using a random walk algorithm modified by a continuous weighting scheme to model the imaginary time evolution described above by eq 6. At the end of the simulation, E_{ref} gives an estimate of the ground-state energy. The accuracy of the method is determined by the size of the time step $\Delta\tau$, the propagation time, and the number of points in $3N$ space ("replica"), representing the wave function.

In practical terms, we perform the simulations using our own algorithm with a fixed geometry for each monomer in the cluster, in order to remove the intramolecular degrees of freedom.[27] This rigid-body DMC (RB-DMC) concept was first introduced by Buch.[28] By focusing on the intermolecular modes of a larger time scale, this method increases the efficiency of the simulation and allows larger time steps to be used compared to an all-atom simulation. Note that this technique is exact within the above rigid-body approximation, and that therefore the result depends only on the quality of the potential energy surface.

It is important to note that, in this approach, there is no account for the deformation of the monomers or the contribution of internal vibrational modes to the intermolecular vibrational ground state. In our case, the phenol molecule is treated as a rigid monomer which is a reasonable starting assumption, owing to the size of the clusters investigated, and our study is only valid within this frame. The restriction of the simulation to contributions from intermolecular nature imposes some limitation on the scope of our results, but it would be very difficult to include the intramolecular modes within the algorithm without an important modification of the RB-DMC theory.

III. Computational Details

A. Potential Energy Surface for Phenol−Water Complexes. The intermolecular potential we use for the phenol (P)−water (W) interaction is based on a rigid-body site−site Coulomb plus Lennard-Jones model expressed as

$$E_{\mathrm{inter}}(P-W_k) = \sum_{i\in P}\sum_{j\in W_k} \frac{q_i q_j e^2}{r_{ij}} + \frac{A_{ij}}{r_{ij}^{12}} - \frac{C_{ij}}{r_{ij}^{6}} \qquad (7)$$

where $A_{ij} = \sqrt{A_{ii}A_{jj}}$ and $C_{ij} = \sqrt{C_{ii}C_{ii}}$ with $A_{ii} = 4\epsilon_i\sigma_i^{12}$ and $C_{ii} = 4\epsilon_i\sigma_i^{6}$. The i and j indices refer to all the phenol and water sites, respectively.

The values of the ii parameters are taken from the optimized potential for liquid simulations (OPLS) model for phenol.[29] The jj elements are the TIP4P[30] four-site model data (three atomic sites plus an extra charge located 0.15 Å from the oxygen on the C_2 axis) for water.

TABLE 1: Potential Energy Parameters Describing Phenol−Phenol and Water−Water Interactions[a]

molecule	type of site	ϵ_i(kcal mol^{-1})	σ_i(Å)	q_i (e)
phenol[b]	C (ar)	0.070	3.55	−0.115
	H (ar)	0.030	2.42	0.115
	O (H)	0.170	3.07	−0.585
	H (O)	0.000	0.00	0.435
	C (OH)	0.070	3.55	0.150
water[c]	O	0.155	3.15	0.000
	H	0.000	0.00	0.520
	M	0.000	0.00	−1.040

[a] The fixed geometries of each monomer are as follows: d(C−C) = 1.40 Å, d(C−H) = 1.08 Å, d(C−O) = 1.36 Å, d(O−H) = 0.96 Å, ∠CCC = ∠CCH = ∠CCO = 120°, ∠COH = 109° for the phenol molecule; d(O−H) = 0.9572 Å, ∠HOH = 104.52° for the water molecule, with an extra site (M) displaced from the oxygen by 0.15 Å on the C_2 axis toward the hydrogen atoms. [b] Reference 29. [c] Reference 30.

The water−water interaction is then calculated with a TIP4P model using a similar formula:

$$E_{\mathrm{inter}}(W_l - W_m) = \sum_{i\in W_l}\sum_{j\in W_m} \frac{q_i q_j e^2}{r_{ij}} + \frac{A_{ij}}{r_{ij}^{12}} - \frac{C_{ij}}{r_{ij}^{6}} \qquad (8)$$

Finally, the total interaction energy (D_e) for a system composed of a phenol molecule and n water molecules is given by

$$E_{\mathrm{inter}}(\mathrm{system}) = \sum_{k=1}^{n} E_{\mathrm{inter}}(P - W_k) + \sum_{l=1}^{n}\sum_{m>l}^{n} E_{\mathrm{inter}}(W_l - W_m) \qquad (9)$$

The numerical details regarding all the parameters used are displayed in Table 1. Note that this potential energy surface contains only two-body (pairwise) terms and does not explicitly include any higher many-body contributions. Although this type of potential is simple, it is widely used in the modeling of organic molecules. The recent availability of spectra for hydrated molecules such as phenol−$(H_2O)_n$, abbreviated hereafter to P−W$_n$, presents a new opportunity for testing the accuracy of these potential energy surfaces (PES), and that is emphasized here.

B. Ab Initio Calculations. In addition, we perform ab initio calculations using Gaussian98[31] on SGI Power-Challenge and Origin 2000 computers. Density functional theory (DFT) calculations are performed with the hybrid B3LYP functional, a three-parameter functional developed by Becke (B),[32] which uses the Lee−Yang−Parr (LYP)[33,34] correlation functional in its Gaussian98 implementation. MP2 calculations are performed using a direct algorithm and include all core electrons. All geometries are optimized in redundant coordinates using the GDIIS algorithm[35] with analytical gradients. Basis-set superposition error (BSSE) is accounted for using the full counterpoise method, including monomer deformations. The infrared frequency calculations are performed using analytical Hessians without a scaling factor.

C. RB-DMC Simulations. The initial vibrational wave function is first approximated by a Dirac function localized at the global minimum for each system, since in most cases there is a high probability that this minimum will contribute significantly to the ground state. The first stage in our RB-DMC simulation of the vibrational ground state of a cluster, namely the equilibration, is performed by diffusing 1000 "replicas" (geometries), using time steps of 60 au, until the standard error on the ground-state energy is smaller than 0.75%. Afterward,

TABLE 2: Comparison of Different Methods To Estimate the Isomer Ordering of Phenol−H_2O[a]

	interaction energy (cm^{-1})			
method	isomer **1a**	isomer **1b**	isomer **1c**	water dimer
OPLS//OPLS	−2540.3	−2137.6	−1263.2	−2191
MP2/6-31G(d,p)[b]	−2361.5	−1179.6	−640.9	−1628.7
MP2/6-311++G(d,p)[c]	−2070.5	−1331.6	−896.7	−1558.8
MP2/6-31G(d,p)//OPLS	−2290.1	−759.7	−389.5	−1409.7
MP2/6-311++G(d,p)//OPLS	−1906.6	−830.6	−557.2	−1228.6
B3LYP/6-31G(d,p)[c]	−2502.4	−1125.0	−471.5	−1770.8
B3LYP/6-311++G(d,p)[c]	−2141.1	−1309.9	−612.5	−1756.6
B3LYP/6-31G(d,p)//OPLS	−2427.8	−769.0	−53.7	−1651.4
B3LYP/6-311++G(d,p)//OPLS	−1967.1	−829.2	−8.1	−1499.8

[a] All ab initio interaction energies are corrected for BSSE using the counterpoise method including monomer deformation. Note that all minima have been characterized by a Hessian calculation. [b] Full Cartesian optimization (maximum gradient below 10^{-5} hartree/bohr). [c] Full redundant coordinate optimization (maximum gradient below 10^{-5} hartree/bohr).

the resulting ensemble of replica is propagated, using time steps of 15 au, until the ground-state energy is converged to a standard error of 0.1% for P−W_n ($n = 2-4$) and 0.05% for P−W_5. This constitutes the actual RB-DMC simulation where the energy, the rotational constants, the structure, and the wave function of the vibrational ground state are calculated. Note that the rotational constants and the vibrationally averaged values are computed by using the descendant weighting method.[36]

All RB-DMC calculations are performed using our own code "Xdmc", which implements our latest rigid-body algorithm and allows us to visualize the wave functions using a one-particle-density method.[27] Indeed, since the RB-DMC method computes the wave function for each atom in the system, it is easy to calculate a vibrational probability density for the atoms with identical masses. This one-particle density is then very convenient to display as an isosurface in three-dimensional space and allows a detailed representation of the zero-point motion of each group of atoms it represents. Typically, the surfaces used enclose 99.9% of the atomic densities ("H-densities").

IV. Results

A. Phenol−Water. In order to assess the accuracy of the OPLS potential energy surface[29,30] and to check its applicability to RB-DMC calculations on P−W_n clusters, we carry out a set of ab initio calculations using the MP2[37] and DFT/B3LYP methods.

First of all, we need to determine if the π-hydrogen bonded isomer (see Figure 1c) found on the OPLS surface is present at the ab initio level. We optimize the three structures shown in Figure 1 at the MP2 and B3LYP levels of theory, using 6-31G-(d,p) and 6-311++G(d,p) basis sets. Our results are summarized in Table 2 and show that the π structure is indeed a stable minimum with no imaginary frequency at either the DFT or MP2 level. The dissociation energies obtained at the MP2/6-31G(d,p) level are consistent with Feller's calculations.[8] Nevertheless, it is known that basis-set superposition error (BSSE) can be important in hydrogen-bonded complexes,[38] so in this paper we only report results corrected using the counterpoise method, including monomer deformation (see ref 39 for a review).

Since we are aiming at determining relative energies of extended molecular systems, we compare the results of the computationally less demanding B3LYP method to the more involved MP2 approach. We also relate these ab initio results to a mixed procedure, where the energy of a particular isomer is calculated at the MP2 or B3LYP level, using a similar basis set, at a minimum geometry computed on the OPLS surface. We call these procedures MP2//OPLS and B3LYP//OPLS respectively to simplify the notation.

An examination of Table 2 reveals that there is a difference between MP2 and B3LYP calculations. Nevertheless, for the geometries involving only "usual" hydrogen bonds—classical hydrogen bond donor or acceptor—the two methods converge toward similar values as the basis set is increased. Indeed, for structures **1a** and **1b** the energies are within ~3% of each other with a 6-311++G(d,p) basis set and BSSE correction. We notice that structure **1a** is the global minimum in all cases and is invariably followed by structure **1b** at every level of theory. This is consistent with the experimental fact that phenol is a stronger acid than water in the gas phase, leading to a strong phenol−donating hydrogen bond and a weaker phenol−accepting hydrogen bond.

In the case of the π-bonded structure, we start to see a rather systematic distinction between the MP2 and the B3LYP results. Although the convergence pattern is similar, we observe a difference of 26−32% between the MP2 and DFT interaction energies for the optimized structure **1c**.

Our mixed procedure performs well for isomer **1a**: regardless of the method we obtain a difference of 3% at the 6-31G(d,p) level and 8% at 6-311++G(d,p). For the second isomer (**1b**), we observe a strong diminution of performance, with a difference of 36% and 38% for MP2 and 32% and 37% for B3LYP. When it comes to the π-bonded structure, the mixed procedure behaves as in the case of isomer **1b** with MP2 (39% and 38% difference) but fails completely to give a reliable estimation of the interaction energy with the B3LYP functional where the differences are 89% and 99%. Nevertheless, with every calculation method the relative energetic ordering of the isomers is always identical and only the ratio between the different interaction energies varies.

To check the applicability of the method to systems containing more than one water molecule, we calculate the interaction energy of the water dimer using the same procedures. Again, there is a difference between the result obtained with the MP2 method and the DFT/B3LYP functional of 9% and 13% for each basis set. The density functional is very close to the complete basis-set limit energy at the CCSD(T) level obtained by Halkier et al.,[41] while the MP2 result is still 200 cm^{-1} above it. With our mixed procedure we obtain a slight deviation for the MP2 results (13% and 21%) and a smaller error for B3LYP (7% and 15%).

The OPLS potential performs well in predicting the ordering of the different isomers, but generally overestimates the bonding energy of each geometry. However, note that this PES is constructed for simulations of the liquid state, a state where the collective forces are usually enhanced with respect to the gas phase. As a consequence, it is to be expected that this potential becomes more accurate as the number of molecules in the system increases.

These findings lead to several conclusions which might be useful in the study of the other isomers. We see that every method gives the same ordering of the three phenol−H_2O isomers, and B3LYP optimization gives similar results to MP2 with a given basis set at a lower computational cost.

Our mixed MP2//OPLS procedure gives reasonable results considering the time-consuming nature of the method and treats the π bonding correctly, but with a given basis set it is less accurate than B3LYP.

TABLE 3: Results for the Phenol−$(H_2O)_n$ (n = 2, 3, 4) Clusters on the OPLS Potential Energy Surface[a]

cluster	rotational constants (MHz)			$\langle d(O-O)\rangle$ (Å)	bonding energy (cm^{-1})
	A	*B*	*C*		
phenol−$(H_2O)_2$ (min)	2636.6	794.6	694.7	2.762	−5984.4
phenol−$(H_2O)_2$ (gs)[b]	2631 ± 9	760 ± 2	656 ± 3	2.844 ± 0.001	−4574 ± 4
phenol−$(H_2O)_3$ (min)	1812.0	570.0	475.8	2.718	−9921.1
phenol−$(H_2O)_3$ (gs)[b]	1847 ± 12	540 ± 3	450 ± 3	2.798 ± 0.001	−7534 ± 7
phenol−$(H_2O)_4$ (min)	1356.8	410.1	327.4	2.712	−13098.9
phenol−$(H_2O)_4$ (gs)[b]	1113 ± 12	489 ± 7	418 ± 8	2.799 ± 0.001	−9839 ± 10

[a] "gs" stands for vibrational ground state. [b] Calculated using rigid-body diffusion Monte Carlo.

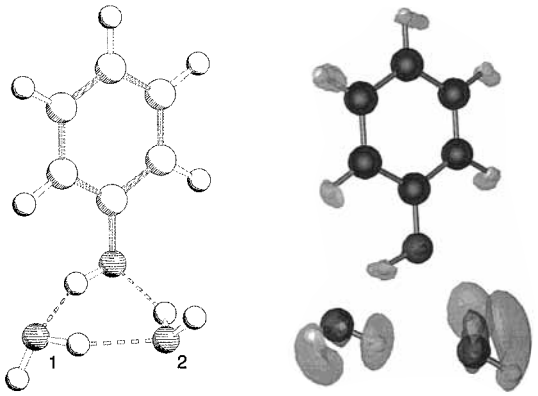

Figure 2. On the left, minimum energy structure of the {Udu} isomer of phenol−$(H_2O)_2$ calculated on the OPLS surface. On the right, corresponding hydrogen-atom density (light surface) and oxygen-atom density (dark surface) for the vibrational ground state of this cluster calculated by RB-DMC.

In the light of these results, we choose the mixed MP2/6-311++G(d,p)//OPLS procedure with BSSE correction to estimate the energy of the phenol−water complexes and their relative ordering. We decide to use a B3LYP/6-311++G(d,p) redundant-coordinate optimization with an analytical frequency calculation to compute the infrared vibrational spectra of P−W_5 isomers, due to the large size of these clusters.

B. Phenol−Water$_2$. The results obtained for P−W_2 are summarized in Table 3. Both the structure of the vibrational ground state obtained by RB-DMC and the minimum are very similar to the parent $(H_2O)_3$ cluster. In both cases, the two water molecules are hydrogen bonded to the −OH group of the phenol molecule, with the three oxygen atoms lying on a plane and forming a triangular system (see Figure 2); the phenol molecule itself acts as a "phenyl-substituted water molecule". Ab initio Hartree−Fock studies of this cluster[7,9,11,12] show that this ring form is indeed the most stable, and its calculated spectrum fits the experimental infrared data[2−4,6,7,9,11,12] very well.

P−W_2 possesses a lower symmetry than the water trimer due to the presence of the phenyl ring; therefore the complex has a series of distinguishable conformers, which we can describe by noting simply the position of the hydrogen atoms above (u) or below (d) the oxygen plane and using a capital letter for the phenol molecule. This notation was first defined by Schütz et al.[43] to describe the water trimer. For example, we can write the four possible minima with the phenyl ring pointing upward as {Udu}, {Uud}, {Udd}, and {Uuu}. Note that there are four other combinations with the phenyl ring pointing downward, which are the enantiomers of the {U*xx*} conformers. We find that {Udu} is the most stable conformation on the OPLS surface, in full agreement with the ab initio calculations.

First, our RB-DMC results show that the vibrationally averaged oxygen−oxygen distances point to a cyclic structure of the hydrogen-bonded network, in agreement with most of the theoretical and experimental observations. Second, the analysis of the three-dimensional probability of finding a hydrogen atom (H-density), shown in Figure 2, tells us that the protruding hydrogen atoms are very delocalized and flip from pointing upward to pointing downward and vice versa. This easy motion partly removes the asymmetry of the cycle, by effectively mixing the {u/d} isomers together in a quantum mechanical way. This result is in agreement with the ab initio work of Leutwyler et al.,[9] in which they find that the interconversion barriers between isomers at the Hartree−Fock level are very small. In this respect, the behavior of this system is reminiscent of the delocalized nature of the water trimer.[43−45] Nevertheless, although there seems to be a slight Up/Down delocalization of the phenol ring, there are no real signs of delocalization over the {D*xx*} and {U*xx*} family of isomers.

An examination of the three-dimensional oxygen-atom density (O-density) shows that there is a slight difference between the two water molecules. If we focus on the hydrogen bonds directly involving the −OH group of the phenol molecule, we notice that while the oxygen atom of the proton-accepting water molecule (water 1 in Figure 2) is fairly localized, the oxygen atom of the proton-donating water molecule (water 2 in Figure 2) shows signs of delocalization (larger lobe on Figure 2). This behavior can be explained in terms of relative bond strength: as we showed earlier for P−W_1 (see section IVA and Table 2), it is energetically more favorable for a water molecule to be in a hydrogen-accepting position (geometry **1a**) than a hydrogen-donating position (geometry **1b**) with respect to the alcohol group. Therefore, in P−W_2, the strong interaction forces water 1 to stay localized, whereas the relative weakness of the second interaction causes water 2 to be more affected by the zero-point delocalization. As a result, there is a slight asymmetry in the extent of the delocalization for this complex, and the cluster resembles a P−W_1 complex with an extra water molecule attached to its side. To support this fact, we notice that an analysis of the oxygen−oxygen distances in P−W_2 reveals that the distances involving water 1 are shorter than the distance between water 2 and the phenol molecule, both in the ground state and in the minimum-energy structure. The difference in bond length persists at the ab initio level, as demonstrated by the HF/6-31++G(d,p) calculation of Gerhards et al.[11] Note that this asymmetry is not present in the vibrational ground state of the water trimer, where all water molecules are equivalent.

The lengthening of the average oxygen−oxygen distance by about 0.08 Å in the vibrational ground state (see Table 3) is typical of vibrational zero-point effects and results in a change in the value of the rotational constants. Nevertheless, our values at both the minimum and the ground state agree well with the Hartree−Fock calculations of Gerhards et al.,[11] and this is due to the strong directional effect of the phenol molecule which contributes much more to the magnitude of the rotational constants than the water molecules do. It is also important to notice that the water molecules never interact with the phenyl

TABLE 4: Phenol−$(H_2O)_n$ (n = 2−5) Interaction Energies (D_e) and Harmonic Zero-Point Energies (ZPE) for Each Minimum at Various Levels of Theory

		D_e (cm^{-1})			harmonic ZPE (cm^{-1})	
cluster	isomer	OPLS	HF/6-31G(d,p)	MP2[a]	OPLS	HF/6-31G(d,p)
phenol−$(H_2O)_2$	{Udu}	−5 984.4	−6 098[b]	−5 712[c]	1548.9	1689[b]
phenol−$(H_2O)_3$	{Udud}	−9 921.1	−10 090[d]	−9 965[d]	2581.7	2623[e]
phenol−$(H_2O)_4$	{Ududu}	−13 098.9	−13 380[f]	−13 384[f]	3485.4	3427[f]
phenol−$(H_2O)_5$	cyclic	−15 974.9	−16 339[f]	−16 270[f]	4283.0	4173[f]
phenol−$(H_2O)_5$	book-*exo*	−16 391.7	−	−	4625.6	−
phenol−$(H_2O)_5$	prism	−16 442.5	−	−	4879.5	−
phenol−$(H_2O)_5$	cage	−16 777.2	−17 195[f]	−16 342[f]	4919.3	4678[f]
phenol−$(H_2O)_5$	book-*endo*	−17 031.9	−16 908[f]	−16 616[f]	4797.1	4510[f]

[a] MP2/6-31G(d,p)//HF with BSSE correction. [b] Reference 9. [c] Reference 11. [d] Reference 10. [e] Intramolecular frequencies scaled by 0.9 (from ref 10). [f] Reference 13.

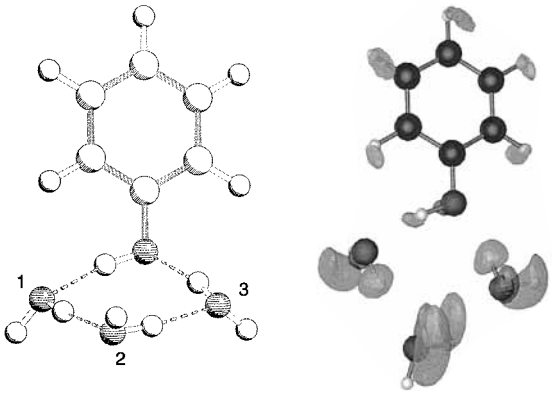

Figure 3. On the left, minimum energy structure of the {Udud} isomer of phenol−$(H_2O)_3$ calculated on the OPLS surface. On the right, corresponding hydrogen-atom density (light surface) and oxygen-atom density (dark surface) for the vibrational ground state of this cluster calculated by RB-DMC.

ring, at least in the ground state. This is due to the sizable energy difference between a structure involving a π-hydrogen bond and the low-energy isomers; consequently, this region of the PES does not have any effects on the ground state of this cluster. This fact was also reported by Gerhards et al.[11]

It is of interest to note that the interaction energy calculated with the OPLS force field (see Tables 3 and 4) is very close to the energies calculated at the HF/6-31G(d,p) level[9,11] (2% difference) or even the MP2/6-31G(d,p)//HF level with BSSE correction[11] (5% difference). One can also note that the harmonic intermolecular zero-point energy is very similar in the case of OPLS and HF/6-31G(d,p) (about 8% difference), even if the ab initio result includes the difference of intramolecular ZPE for each monomer.

C. Phenol−$Water_3$. The RB-DMC results obtained for P−W_3 are reported in Table 3. Here again the overall structure of the complex both at the minimum and in the vibrational ground state resembles the parent water tetramer of S_4 symmetry, where one hydrogen atom is substituted by a phenyl ring (see Figure 3). This geometry is consistent with all the experimental data[2−7,10,12,13] and the ab initio work at various levels.[10,12,13] The four oxygen atoms lie approximately on a plane, allowing us to describe the different conformers using the same notation as above. The global minimum on the OPLS and ab initio surfaces is the {Udud} isomer. Other cyclic isomers are possible, differing only by the position in the protruding hydrogen atoms, as in the case of P−W_2. Bürgi et al.[10] located four of them, which they calculated to be at least 175 cm^{-1} above the global minimum at the HF/6-31G(d,p) level.

As previously, we observe a lengthening of the mean oxygen−oxygen distance by 0.08 Å in the vibrational ground state (see Table 3), which in turn affects the values of the rotational constants. Again, our values are close to that obtained at the HF/6-31G(d,p) level by Bürgi et al.[10] Note that, here, the phenyl group plays the same directional role as for P−W_2, which explains the agreement between the different calculations. One interesting feature of this system is the existence of a chiral isomer to {Udud}, namely {Dudu}; it has been suggested that there could be an interconversion between these two forms in the ground state.[10] A close examination of the three-dimensional probability density for the hydrogen atoms produced by the RB-DMC calculation (see Figure 3) shows that there is a free flipping motion of the protruding hydrogen atoms, as is the case for the water tetramer. This suggests that the isomerization barriers between the cyclic minima of the cluster are small, as was the case for P−W_2. As a result of the analysis of the H-density, we observe a strong delocalization of the phenyl group, although this does not result in the aforementioned {Udud}→{Dudu} isomerization. This unexpected mobility of the phenyl group was also pointed out by Bürgi et al.[10] on the basis of a harmonic normal-mode analysis at the HF/6-31G(d,p) level.

The P−W_3 cluster has a vibrational ground state which undergoes more zero-point delocalization than its water cluster analogue $(H_2O)_4$; an examination of the O-density shows that the oxygen plane can be twisted to some extent. As was the case for P−W_2, we notice that, in the ground state, the water molecules which are not in a hydrogen-accepting position with respect to the phenol molecule (water 2 and water 3) are prone to large-amplitude motion (see Figure 3). This is consistent with the difference in hydrogen-bond length found for the minimum, also noticed by Bürgi et al.[10] at the HF/6-31G(d,p) level.

As shown in Table 3, the full zero-point energy correction represents 24% of the bonding energy at the minimum on the OPLS surface; this is consistent with the prediction of Bürgi et al.[10] made at the HF/6-31G(d,p) level. They postulated that a full treatment of the anharmonicity should give a result lower than their harmonic ZPE estimation (26% of the bonding energy) and therefore increase the dissociation energy of the cluster. This agreement could, of course, be fortuitous considering the fact that we are not carrying out our calculations on the same potential energy surface. However, in Table 4, we notice a very good agreement between the interaction energy calculated with OPLS and a more elaborate method such as MP2/6-31G(d,p)// HF with BSSE correction[10] (0.4% difference). The same is also true with the harmonic zero-point energy, where we observe a difference of 2% between our result and that published by Bürgi et al., which explains partly the applicability of their predictions to our results.

D. Phenol−$Water_4$. The RB-DMC results obtained for P−W_4 are reported in Table 3. As for the previous clusters, the

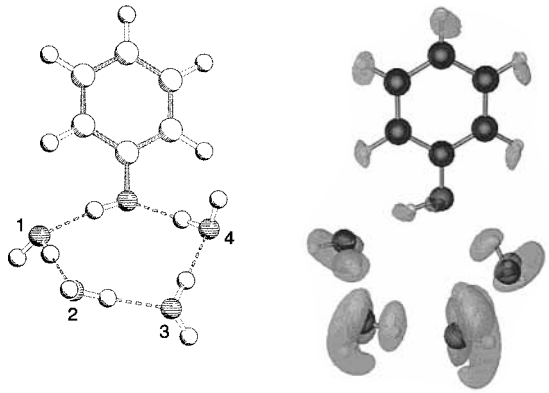

Figure 4. On the left, minimum energy structure of the {Ududu} isomer of phenol$-(H_2O)_4$ calculated on the OPLS surface. On the right, corresponding hydrogen-atom density (light surface) and oxygen-atom density (dark surface) for the vibrational ground state of this cluster calculated by RB-DMC.

structure of this complex is very similar to that of the water pentamer if one replaces the phenyl ring by a hydrogen atom (see Figure 4). The calculations at the HF/6-31G(d,p) level find that a cyclic minimum fits the experimental infrared spectra.[2,3,7,13] Once again, we can use the convention of Schütz et al.[43] to describe the different cyclic isomers. Most of the theoretical work concludes that the {Ududu} cyclic structure is the lowest energy form of the cluster.[7,12] This is equally the case with our calculation on the OPLS surface, where we obtain a slightly nonplanar oxygen cycle, resembling a cyclopentane envelope structure.

By analyzing the HF/6-31G(d,p) geometry published by Jacoby et al. on the Internet (ref 15 in ref 13), we find that their rotational constants are very similar to the ones we obtain for the OPLS minimum. In the vibrational ground state, the phenyl group loses its directional effect and there is now a larger difference between ground-state and minimum values of the rotational constants (from 18% for A to 28% for C). This is due to a significant delocalization of the water molecules furthest away from the phenyl group (water 2 and water 3 in Figure 4).

Our RB-DMC calculation shows that the mean oxygen−oxygen distance still increases upon vibrational averaging by about 0.08 Å, but is very close to the values obtained for $P-W_3$. On the basis of their HF calculations, Burgi et al.[10] noticed that, in the cyclic form of the $P-W_n$ clusters, the mean oxygen−oxygen distance decreases as n increases from 1 to 3. They ascribed this fact to the effect of many-body contributions to the potential energy surface. Our calculations follow this predicted trend quite closely, even if our PES does not explicitly include any many-body term higher than order 2.

The isomerization barriers for the flipping of a hydrogen atom were estimated to be about 150 cm^{-1} at the HF/6-31G(d,p) level by Jacoby et al.[13] An analysis of the H-density for the vibrational ground state (see Figure 4) does indeed show a large delocalization of the "free" protruding hydrogen atoms of the water molecules, and also a slight delocalization of the phenyl group. Note that this motion is of much smaller amplitude than in the $P-W_3$ cluster. As a result of this hydrogen delocalization, a mixing occurs between all the different {u/d} isomers in the vibrational ground state of the complex. This situation is very similar to that of the previous smaller cyclic clusters. The O-density for the $P-W_4$ cluster again shows an asymmetry in the localization of the oxygen atoms of the water molecules (see Figure 4). As was the case for the previous clusters, water 1 is more localized than any other water molecule in the system. The further the water molecules are from the influence of the phenol molecule (water 2 and water 3), the more mobile they become, therefore contributing to the floppiness of the oxygen cycle. Nevertheless, the water molecules do not seem to interact with the phenyl ring.

The comparison of the interaction energy on the OPLS surface with the MP2/6-31G(d,p)//HF results of Jacoby et al.[13] including BSSE correction again shows a good agreement, with only 2% difference (see Table 4). The same is true for the harmonic zero-point energy, where we also observe a difference of 2% from the value published by Jacoby et al.

E. Phenol−Water$_5$. Our results for $P-W_5$ are summarized in Table 5. In the case of this cluster, there is more than one structural motif for the low-lying isomers. A detailed analysis of the PES shows that there are a few families of conformations and, moreover, some of these are related to the water hexamer. We examine only a selection of these low-lying energy structures (depicted in Figure 5), which contains our best estimate of the global minimum as well as geometries already reported in the literature.[7,12,13]

We can divide the isomers into two classes: hexamer-like and π-bonded. The hexamer-like structures are similar to the ones encountered in the water hexamer, where one hydrogen atom is replaced by a phenyl ring, and they are formed of two subclasses: the monocyclic complexes and the polycyclic complexes. These two subclasses contain most of the $P-W_5$ structures described in the literature so far.[3,4,6,12] In the monocyclic family we find the cyclic {Ududud} isomer. The polycyclic class contains the prism, the cage, and the book-*exo* isomers. The π-bonded structures have the common feature of a π-hydrogen bond between a water molecule and the phenyl ring and have already been considered by the Kleinermanns group.[7,13] This class possesses a variety of isomers which often differ only in the position of a free-water −OH bond and therefore have relatively similar energies. In this study, we choose as a typical member of this class the global minimum on the OPLS potential energy surface, which we name the book-*endo* structure. This structure looks like a book-*exo* isomer in which the water molecules are folded back onto the phenyl ring.

The relative energetic ordering of each isomer on the OPLS surface is shown in Figure 5. We can see that every isomer is relatively close in energy to its neighbors and that the energy range spanned by the five isomers shown is only about 1000 cm^{-1}. Moreover, the structural changes that occur within these limits are quite dramatic and complicate the problem of determining reliably the geometry of the global minimum for this cluster. Calculations at the ab initio level seem to disagree on the nature of this global minimum: Watanabe[12] finds the cyclic structure to be lowest at the HF/6-31G level, but Jacoby[13] finds that, at the MP2/6-31G(d,p)//HF level with BSSE correction, the book-*endo* isomer is the lowest.

Our results for the minima of the cage and the book-*endo* isomers compare well with the HF/6-31G(d,p) structures published by Jacoby et al. on the Internet (ref 15 in ref 13). The OPLS minima and their published structures have similar rotational constants. We also observe a very good agreement between the interaction energy of all isomers calculated on the OPLS surface and the MP2/6-31G(d,p)//HF results published by Jacoby et al.,[13] with only 2−3% difference, and the same is true for the harmonic zero-point energy (see Table 4). This similarity further validates the use of the PES for the RB-DMC simulation of this cluster.

The RB-DMC calculation of the vibrational ground state, starting from each of the different isomers depicted in Figure 5, reveals that most of these structures are unstable with respect

TABLE 5: Results for the Phenol−$(H_2O)_5$ Isomers[a]

	rotational constants[b] (MHz)			bonding energy (cm^{-1})		
isomer	*A*	*B*	*C*	OPLS	MP2[c]	B3LYP[d]
cyclic (min)	814.7	345.8	275.3	−15 974.9	−13 038.0	−15 531.4
book-*exo* (min)	1272.3	283.1	245.8	−16 391.7	−12 548.2	−15 310.4
prism (min)	1134.9	394.2	366.2	−16 442.5	−12 093.4	−
cage (min)	1555.7	278.8	266.9	−16 777.2	−12 422.0	−15 356.8
book-*endo* (min)	847.2	548.7	486.3	−17 031.9	−12 658.1	−15 315.4
book-*endo* (gs)[e]	796 ± 1	518 ± 1	448.4 ± 0.9	−12 427 ± 6	−	−

[a] "gs" stands for vibrational ground state. [b] Calculated on the OPLS potential energy surface. [c] Calculated using the mixed MP2/6-311++G(d,p)//OPLS procedure with BSSE correction. [d] Full redundant coordinate optimization at the B3LYP/6-311++G(d,p) level, corrected for BSSE (including monomer deformation). [e] Calculated using rigid-body diffusion Monte Carlo on the OPLS surface.

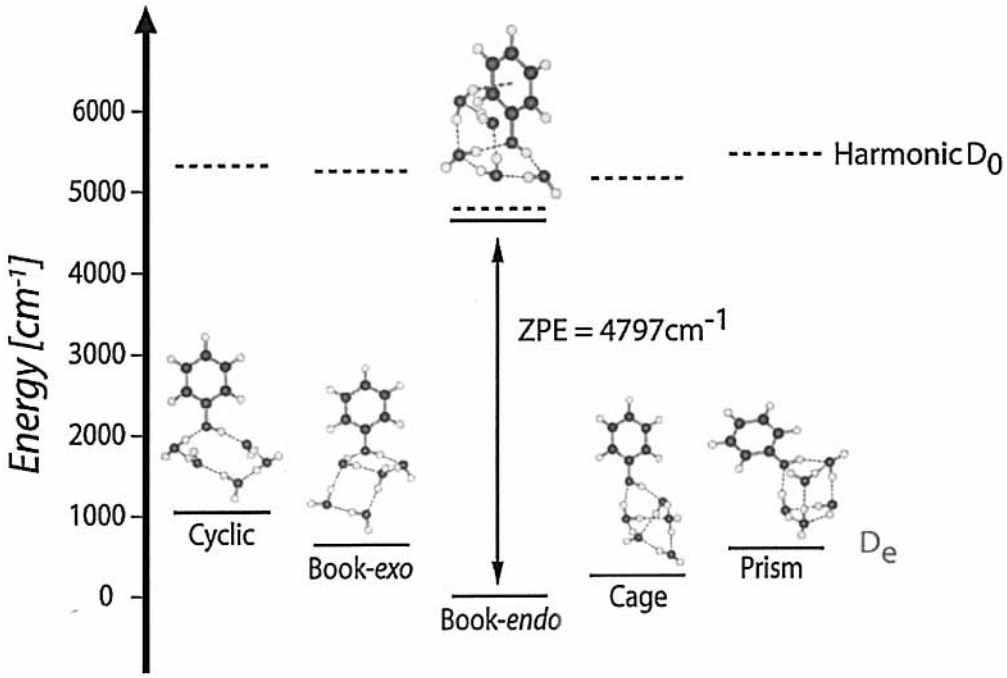

Figure 5. Minimum energy structures and energetic ordering of selected isomers of phenol−$(H_2O)_5$ calculated on the OPLS surface. All energies are relative to the interaction energy (D_e) of the book-*endo* isomer. The absolute D_e values are reported in Table 5. The plain lines are the various D_e, the dashed lines are the harmonic approximation to the dissociation energies (D_0), and the exact D_0 calculated by RB-DMC is indicated for the Book-*endo* isomer by an unbroken line.

to zero-point energy correction, except for the book-*endo* isomer. Indeed, all isomers ultimately diffuse toward the global minimum and end up localized about the lowest energy structure on the PES. Therefore, as was the case for the water hexamer,[17] we are in a situation where the ground state of the system is completely dominated by the lowest energy region of the potential energy surface, here the book-*endo* isomer.

Similarly to the smaller P−W_n clusters, the vibrational averaging increases the mean oxygen−oxygen distance by 0.08 Å. This lengthening produces a decrease of about 6.5% on average for all rotational constants. The directional effect of the phenol molecule is visibly diminished and the water molecules play a more important part in the determination of the values of the rotational constants *A*, *B*, and *C*.

An analysis of the hydrogen-atom density shows that the hydrogen-bonded network is stable, with the nonbonded −OH groups undergoing wide-amplitude motion (see Figure 6). This delocalization effectively mixes the various {u/d} isomers of the π-bonded class, as it did in the ground state of the smaller phenol−water clusters. Note that the −OH bond of water 4 which points toward the phenyl ring is fairly localized above the ring, showing that the π-hydrogen bond is a stable feature of the vibrational ground state.

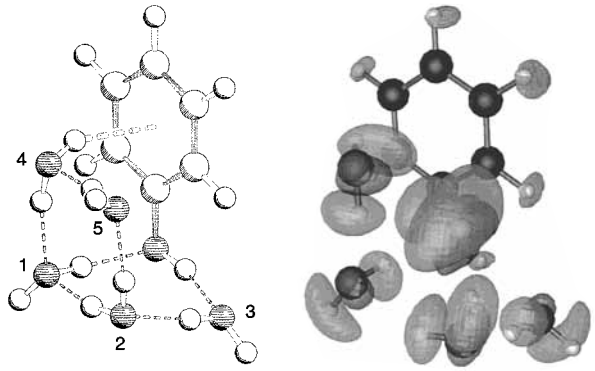

Figure 6. On the left, minimum energy structure of the book-*endo* isomer of phenol−$(H_2O)_5$ calculated on the OPLS surface. On the right, corresponding hydrogen-atom density (light surface) and oxygen-atom density (dark surface) for the vibrational ground state of this cluster calculated by RB-DMC.

There is a difference between the water molecules depending on their function in the hydrogen-bonded network. The two double-donor molecules, water 2 and water 4 (one of which makes the π bond), have hydrogen atoms that are midway between a free and a hydrogen-bonded proton, if we compare them to the single donors water 1 and water 3. Note also that

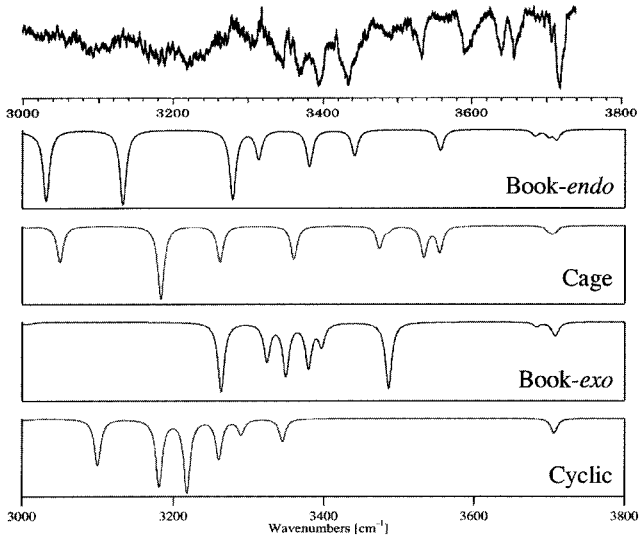

Figure 7. Ab initio B3LYP/6-311++G(d,p) infrared spectra of the OH stretch region of selected isomers of phenol$-(H_2O)_5$ compared with the experimental spectrum of ref 3 (top spectrum). To make the comparison easier, each calculated spectrum is shifted by -179.22 cm^{-1} and we assumed a Lorentzian line shape of fwhm $=$ 10 cm^{-1}.

the two hydrogen atoms of the double-donor molecules have a slightly more symmetric behavior than in the single-donor case. As was the case for the smaller clusters, water 5, which is the furthest away from the phenol molecule, has the hydrogen atoms with the most delocalized character. We also notice a slight delocalization of the phenyl ring about its equilibrium position, but this does not result in any {U/D} isomerization.

The oxygen density exhibits features similar to those shown previously in the smaller clusters. In the direct proximity of the phenol molecule, we notice that water 1 is more localized than water 3, as was the case for the smaller P$-$W$_n$ clusters. Further away from the phenol molecule, the water molecule 4, which is undergoing π-hydrogen bonding to the phenyl ring, is only slightly delocalized and seems to be held in place by both the hydrogen-bond interactions with water 1 and water 5 and the π-hydrogen bond. The two remaining water molecules (water 2 and water 5) are showing signs of delocalization, which is consistent with a weaker attraction from the phenol molecule as the distance from it increases. The main difference from the earlier cyclic systems is that in general the whole, rather than part, of the hydrogen-bonded network is delocalized about its equilibrium position.

Most experimental papers[3,4,6,7,13] agree that the infrared spectrum recorded for P$-$W$_5$ is very different from the infrared spectra of the smaller cyclic clusters, and does not exhibit any of the usual features characteristic of a cyclic structure. This observation is further consolidated by the fact that the theoretical IR spectrum of the cyclic isomer, calculated at various levels, does not correlate with experimental data (see Figure 7, for example).

In order to compare our results with the experimental data available, we decide to perform DFT calculation on four low-lying isomers of P$-$W$_5$, namely the cyclic, book-*exo*, cage, and book-*endo* structures. As discussed in section IV.A, the IR frequencies obtained at the B3LYP/6-311++G(d,p) level are of a quality similar to that of a MP2 analysis with the same basis set, but at a smaller computational cost.

Our simulated infrared spectra are shown in Figure 7, along with the experimental jet-cooled spectrum of Watanabe et al.[3] for P$-$W$_5$. To make the comparison easier, we give each theoretical line a Lorentzian line shape of fwhm $=$ 10 cm^{-1} and shift all simulated spectra so that the $-$OH stretch of isolated B3LYP/6-311++G(d,p) phenol matches Watanabe's reported experimental value (total shift of -179.22 cm^{-1}).

According to the experimental and theoretical data on the phenol$-$water complexes, cyclic structures exhibit a characteristic feature in their vibrational spectra. Indeed, the gap between the hydrogen-bonded $-$OH stretch band and the free $-$OH stretch band is often important in these types of structure (at least 100 cm^{-1} in P$-$W$_2$, for example), and grows with cluster size. This gap in the spectrum is commonly named the "window region".[6]

We notice a striking difference between the simulated spectrum of the cyclic isomer in Figure 7 and the spectrum in the experiment. As expected, the cyclic form has a wide "window region" (3400$-$3700 cm^{-1}), and therefore does not match any of the bands immediately following the bonded $-$OH stretch. The spectrum of the book-*exo* isomer offers a reasonable match for the four bands around 3400 cm^{-1} but lacks any significant features in the window region.

The cage isomer was proposed by a number of authors,[3,4,6,12] as the structure which best explains the experimental spectrum. Although it possesses more features in the window region, which can be attributed to double-donor water molecules, they are still too widely spaced to explain all the experimental data. We notice the correct presence of a doublet around 3500 cm^{-1}, but the following free $-$OH stretch region (near 3400 cm^{-1}) is not faithfully reproduced.

The book-*endo* structure was also considered by Jacoby et al.[13] as a possible match for their intermolecular dispersed fluorescence spectrum of P$-$W$_5$. Our calculation shows that this isomer has a spectrum similar to that of the cage structure, but with more matching features in the 3400 cm^{-1} region. It lacks the doublet present in the previous spectrum but exhibits two small bands near 3700 cm^{-1} which we attribute to the π-bonding of one of the water molecules to the phenyl ring. This assignment is consistent with the work on benzene$-$water clusters by Zwier et al.,[46] who showed that the region from 3600 to 3700 cm^{-1} is typical of water molecules π-bonded to an aromatic ring.

Generally speaking, although the book-*endo* isomer seems a likely candidate, no infrared spectrum, at either the HF/6-31G-(d,p) or B3LYP/6-311++G(d,p) level, completely matches the experimental data, and there is some room for improvement in the simulations of the IR spectrum of this cluster. Nevertheless, there is a noticeable difference in the predicted rotational constants of each isomer (see Table 5), and a microwave spectrum should be able to provide enough data to determine which geometry is seen in a supersonic jet.

If we examine the energetic ordering of the different isomers of P$-$W$_5$, we see a difference between the ab initio methods and the model potential. While OPLS has the book-*endo* structure as the global minimum, both our mixed MP2/6-311++G(d,p)//OPLS procedure and B3LYP/6-311++G(d,p) give the cyclic isomer with minimum energy (see Table 5). However, a cyclic structure does not explain the experimental infrared spectrum. Still, it is important to notice that the energies calculated for the different isomers at the B3LYP level all lie within a 220 cm^{-1} range, which is well below the commonly accepted accuracy of the method. Resolving such a small difference in interaction energy represents a major challenge given the size of the system and cannot be done with our present computational resources. Therefore, the energetic ordering of these isomers still remains uncertain.

V. Conclusion

Using ab initio methods, we demonstrated the existence of a π-hydrogen bonded structure for phenol$-H_2O$. We performed RB-DQMC simulations of the vibrational ground state of phenol$-W_n$ ($n = 2-5$) clusters on the OPLS potential energy surface, showing that for $n \leq 4$ all the lowest energy forms of the clusters assume a cyclic structure, reminiscent of the parent $(H_2O)_{n+1}$ water cluster. We assessed the importance of quantum delocalization and zero-point effects for these clusters, which leads to a lengthening of the oxygen−oxygen distances in the vibrational ground state and affects the values of the rotational constants of the cluster. The hydrogen-atom densities show clearly that the hydrogen-bonded network is stable in all cases and that the −OH bonds not taking part in the hydrogen bonding undergo heavy delocalization, whereby the different torsional isomers of a particular cluster are mixed together.

In the case of $P-W_5$ with the OPLS potential, we observed that vibrational zero-point effects are significant, and a π-hydrogen bonded geometry has the vibrational ground state with minimum energy. Indeed, the structure of the book-*endo* isomer, which has the most similarities with the vibrational ground state, provides a reasonable match with the experimental infrared spectrum when calculated using density functional theory at the B3LYP/6-311++G(d,p) level. Nevertheless, the small energy separation between the different isomers is pushing the B3LYP method to its limits and the accuracy of the energetic ordering cannot be guaranteed at this level. Consequently, it is quite possible that, due to the proximity of these low-energy structures, the experimental infrared spectrum reflects contributions from several isomers.

While investigating the energetics of phenol−water complexes, we found that the OPLS surface gives interaction energies that are often within 3% of ab initio results at the HF/6-31G(d,p) level or even MP2/6-31G(d,p)//HF level with BSSE correction. This similarity is also valid for the harmonic vibrational zero-point energies, which shows that the OPLS potential energy surfaces are a reasonable starting point for studying clusters where water interacts with organic molecules.

Acknowledgment. This work is supported by the Swiss National Science Foundation (83EU-048880) and the Engineering and Physical Sciences Research Council. R. Thompson is gratefully acknowledged for proofreading the manuscript.

References and Notes

(1) Benoit, D. M.; Chavagnac, A. X.; Clary, D. C. *Chem. Phys. Lett.* **1998**, *283*, 269.
(2) Stanley, R. J.; Castleman, Jr., A. W. *J. Chem. Phys.* **1991**, *94*, 7744.
(3) Watanabe, H.; Ebata, T.; Tanabe, S.; Mikami, N. *J. Chem. Phys.* **1996**, *105*, 408.
(4) Ebata, T.; Fujii, A.; Mikami, N. *Int. J. Mass Spectrom.* **1996**, *159*, 111.
(5) Ebata, T.; Mizuochi, N.; Watanabe, T.; Mikami, N. *J. Phys. Chem.* **1996**, *100*, 546.
(6) Ebata, T.; Fujii, A.; Mikami, N. *Int. Rev. Phys. Chem.* **1998**, *17*, 331.
(7) Roth, W.; Schmitt, M.; Jacoby, C.; Spangenberg, D.; Janzen, C.; Kleinermanns, K. *Chem. Phys.* **1998**, *239*, 1.
(8) Feller, D.; Feyereisen, M. W. *J. Comput. Chem.* **1993**, *14*, 1027.
(9) Leutwyler, S.; Bürgi, T.; Schütz, M.; Taylor, A. *Faraday Discuss.* **1994**, *97*, 285.
(10) Bürgi, T.; Schütz, M.; Leutwyler, S. *J. Chem. Phys.* **1995**, *103*, 6350.
(11) Gerhards, M.; Kleinermanns, K. *J. Chem. Phys.* **1995**, *103*, 7392.
(12) Watanabe, H.; Iwata, S. *J. Chem. Phys.* **1996**, *105*, 420.
(13) Jacoby, C.; Roth, W.; Schmitt, M.; Janzen, C.; Spangenberg, D.; Kleinermanns, K. *J. Phys. Chem. A* **1998**, *102*, 4471.
(14) Courty, A. Les liaisons hydrogène dans les agrégats molécule aromatique-solvant polaire: Structure, énergetique et réactivité. Thesis, Université Paris XI Orsay, 1997.
(15) Courty, A.; Mons, M.; Dimicoli, I.; Piuzzi, F.; Brenner, V.; Millié, P. *J. Phys. Chem. A* **1998**, *102*, 4890.
(16) Gregory, J. K.; Clary, D. C. *Mol. Phys.* **1996**, *88*, 33.
(17) Liu, K.; Brown, M. G.; Carter, C.; Saykally, R. J.; Gregory, J. K.; Clary, D. C. *Nature* **1996**, *381*, 501.
(18) Gregory, J. K.; Clary, D. C. *J. Phys. Chem.* **1996**, *100*, 18014.
(19) Gregory, J. K.; Clary, D. C. *J. Phys. Chem. A* **1997**, *101*, 6813.
(20) Atwood, J. L.; Hamada, F.; Robinson, K. D.; Orr, G. W.; Vincent, R. L. *Nature* **1991**, *349*, 683.
(21) Suzuki, S.; Green, P. G.; Bumgarner, R. E.; Dasgupta, S.; Goddard III, W. A.; Blake, G. A. *Science* **1992**, *257*, 942.
(22) Gutowsky, H. S.; Emilsson, T.; Arunan, E. *J. Chem. Phys.* **1993**, *99*, 4883.
(23) Gregory, J. K.; Clary, D. C. *Chem. Phys. Lett.* **1994**, *288*, 547.
(24) Anderson, J. B. *J. Chem. Phys.* **1975**, *63*, 1499.
(25) Suhm, M. A.; Watts, R. O. *Phys. Rev.* **1991**, *204*, 293.
(26) Kosztin, I.; Faber, B.; Schulten, K. *Am. J. Phys.* **1996**, *64*, 633.
(27) Benoit, D. M.; Clary, D. C. Submitted for publication.
(28) Buch, V. *J. Chem. Phys.* **1992**, *97*, 726.
(29) Jorgensen, W. L.; Nguyen, T. B. *J. Comput. Chem.* **1993**, *14*, 195.
(30) Jorgensen, W. L.; Chandrasekhar, J.; Madura, J. D.; Impey, R. W.; Klein, M. L. *J. Chem. Phys.* **1983**, *79*, 926.
(31) Frisch, M. J.; et al. *Gaussian98*, Revision A.3; Gaussian, Inc.: Pittsburgh, PA, 1998.
(32) Becke, A. D. *J. Chem. Phys.* **1993**, *98*, 5648.
(33) Lee, C.; Yang, W.; Parr, R. G. *Phys. Rev. B* **1988**, *37*, 785.
(34) Miehlich, B.; Savin, A.; Stoll, H.; Preuss, H. *Chem. Phys. Lett.* **1989**, *157*, 200.
(35) Farkas, O.; Schlegel, H. B. *J. Chem. Phys.* **1998**, *109*, 7100.
(36) Kalos, M. H. *Phys. Rev. A* **1970**, *2*, 250.
(37) Møller, C.; Plesset, M. S. *Phys. Rev.* **1934**, *46*, 618.
(38) Xantheas, S. S. *J. Chem. Phys.* **1996**, *104*, 8821.
(39) van Duijneveldt, F. B.; van Duijneveldt-van de Rijdt, F. G. C. M.; van Lenthe, J. H. *Chem. Rev.* **1994**, *94*, 1873.
(40) Tarakeshwar, P.; Choi, H. S.; Lee, S. J.; Lee, J. Y.; Kim, K. S.; Ha, T. K.; Jang, J. H.; Lee, J. G.; Lee, H. *J. Chem. Phys.* **1999**, *111*, 5838.
(41) Halkier, A.; Koch, H.; Jørgensen, P.; Christiansen, O.; Nielsen, I. M. B.; Helgaker, T. *Theor. Chem. Acc.* **1997**, *97*, 150.
(42) Fredericks, S. Y.; Jordan, K. D.; Zwier, T. S. *J. Phys. Chem.* **1996**, *100*, 7810.
(43) Schütz, M.; Bürgi, T.; Leutwyler, S.; Bürgi, H. B. *J. Chem. Phys.* **1993**, *99*, 5228.
(44) Gregory, J. K.; Clary, D. C. *J. Chem. Phys.* **1995**, *102*, 7817.
(45) Sorenson, J. M.; Gregory, J. K.; Clary, D. C. *Chem. Phys. Lett.* **1996**, *263*, 680.
(46) Pribble, R. N.; Zwier, T. S. *Faraday Discuss.* **1994**, *97*, 229.